

Modified PIC Method for Sea Ice Dynamics *

WANG Rui-xue (王瑞学)^a, JI Shun-ying (季顺迎)^{a, b, 1},
SHEN Hung-tao^b and YUE Qian-jin (岳前进)^a

^a State Key Laboratory of Structural Analysis for Industrial Equipment,
Dalian University of Technology, Dalian 116023, China

^b Department of Civil and Environmental Engineering, Clarkson University, Potsdam, NY 13699, USA

(Received 31 January 2005; accepted 10 June 2005)

ABSTRACT

The sea ice cover displays various dynamical characteristics such as breakup, rafting, and ridging under external forces. To model the ice dynamic process accurately, the effective numerical modeling method should be established. In this paper, a modified particle-in-cell (PIC) method for sea ice dynamics is developed coupling the finite difference (FD) method and smoothed particle hydrodynamics (SPH). In this method, the ice cover is first discretized into a series of Lagrangian ice particles which have their own sizes, thicknesses, concentrations and velocities. The ice thickness and concentration at Eulerian grid positions are obtained by interpolation with the Gaussian function from their surrounding ice particles. The momentum of ice cover is solved with FD approach to obtain the Eulerian cell velocity, which is used to estimate the ice particle velocity with the Gaussian function also. The thickness and concentration of ice particles are adjusted with particle mass density and smooth length, which are adjusted with the redistribution of ice particles. With the above modified PIC method, numerical simulations for ice motion in an idealized rectangular basin and the ice dynamics in the Bohai Sea are carried out. These simulations show that this modified PIC method is applicable to sea ice dynamics simulation.

Key words: *particle-in-cell; smoothed particle hydrodynamics; sea ice dynamics; numerical simulation*

1. Introduction

Under natural conditions, the sea ice is a mixture of rafted and ridged ice, level ice and open water, and displays various dynamic properties. A series of numerical methods have been developed to simulate the sea ice dynamical process under different scales. Normally, the ice cover is treated as a two dimensional rheological flow, and the Eulerian finite difference (FD) method is applied widely to the polar zone at large scale, and the sub-polar area at meso-scale (Hibler, 1979; Lepparante and Hibler, 1985; Lu *et al.*, 1989; Zhang and Hibler, 1997; Wu *et al.*, 1998). In the solving of advection in the continuity equation by the FD method, the numerical diffusion gives poor prediction of ice edge position (Huang and Savage, 1998). Some researchers developed other Lagrangian methods to overcome the numerical diffusion problem (Shen *et al.*, 2000; Tremblay and Mysak, 1997; Overland *et al.*, 1998; Wang and Ikeda, 2004).

The Discrete Element Model (DEM) was adopted for sea ice dynamics under Lagrangian coordinate at different scales (Shen *et al.*, 1987; Dai *et al.*, 2004; Hopkins, 1996; Hopkins *et al.*,

* This study was financially supported by the National Natural Science Foundation of China (Grant No. 40206004)

1 Corresponding author. E-mail: jisy@dlut.edu.cn

2004). The DEM is a good approach to the study of the mechanisms of ice floe interaction, ice-wave interaction, ice rafting and ridging, but it has not been used for general ice forecasting and long term simulation for its low computational efficiency. As another Lagrangian approach to sea ice dynamics, the Smoothed Particle Hydrodynamics (SPH) was also applied successfully in the river/ sea ice dynamics (Gutfraund and Savage, 1997a, 1997b; Shen et al., 2000; Lindsay and Stern, 2004). The SPH method can simulate the ice edge accurately, avoiding the numerical diffusion problem. Meanwhile, the huge interpolating calculation among particles, especially in the determination of ice strain rate, stress and internal ice force, is very costly. Thus, the computational efficiency of SPH method should be improved for sea ice forecasting and simulation.

The particle-in-cell (PIC) method is a suitable one with a coupling of Eulerian and Lagrangian coordinates. Flato (1993) firstly introduced the PIC method into the sea ice dynamics for the polar zone, and it was found that the PIC method had an obvious advantage in determining the accurate ice edge position. In the PIC method for sea ice simulation, a bi-linear function was adopted to interpolate the ice variables between ice particles and grid nodes. In the previous PIC method, the ice particle did not have concentration, and its area was a feedback variable of the grid concentration, which was adjusted with the critical concentration condition ($A = 1.0$) at grid node (Flato, 1993). Moreover, the concentration of grid node could also be solved with its continuity equation, while the numerical diffusion still appeared in the solution of the continuity equation with the FD method (Huang and Savage, 1998).

In this paper, the PIC method is modified with flexible particles and a Gaussian interpolating function based on the SPH theory. The Gaussian function has smoother continuity and higher precision than the bi-linear function. The ice concentration and thickness of ice particle can be determined with its mass density and smooth length in ice motion. In this modified PIC method, the ice velocity at grid node is determined by solving the momentum equation with FD method. It is faster than the SPH method which has complex iterations in solving strain rate, stress and internal ice force. With this modified PIC method, the ice ridging process in a rectangular zone, and the ice dynamic process in the Bohai Sea are tested. In the two numerical tests, the simulated ice results are in good agreement with the analytical solution and observed data for the Bohai Sea.

2. Basic Equations of Sea Ice Dynamics

2.1 Momentum Equation

The momentum equation for the motion of the ice field is governed by ice interactions, wind and water forces, the Coriolis force, and ocean tilt effect, and can be written as:

$$M \frac{dV}{dt} = -MfK \times V + a + w - Mg \nabla_w + \nabla(h) \quad (1)$$

where, M is the ice mass per unit area, and $M = \rho_i h$, the mean ice thickness $h = Nh_i$, ρ_i being the ice density, h_i being the ice thickness, N being the ice concentration; V is the ice velocity vector; f is the Coriolis parameter; K is a unit vector normal to ice surface; a and w are the air and water

stresses, and here $\tau_a = \rho_a C_a \left| V_{ai} \right| V_{ai}$, and $\tau_w = \rho_w C_w \left| V_{wi} \right| V_{wi}$, in which ρ_a and ρ_w are the densities of air and current, C_a and C_w are the drag coefficients of wind and current, and V_{ai} and V_{wi} are the relative wind and current velocity vectors; g is the acceleration of gravity; h_i is the ice surface height; τ is the ice stress vector.

2.2 Viscous-Plastic Constitutive Model

In the simulation of sea ice dynamics, the ice cover is normally treated as a 2D continuous medium, and the viscous-plastic (VP) constitutive model with elliptical yield curve law is applied most widely (Hibler, 1979). This VP law can be expressed as:

$$\dot{\tau}_{ij} = 2 \eta_{ij} \dot{\epsilon}_{ij} + (\eta_{kk} - P) \dot{\epsilon}_{ij} - P \delta_{ij} / 2 \tag{2}$$

where $\dot{\tau}_{ij}$ and $\dot{\epsilon}_{ij}$ are the 2D stress and strain rate tensor; P is the ice pressure; δ_{ij} is the Kronecker operator; and η_{ij} are the nonlinear bulk and shear viscosities, and can be determined as:

$$\eta_{ij} = (\dot{\tau}_{ij}, P) = \min(P/2, 0), \tag{3}$$

$$\eta_{ij} = \eta / e^2, \tag{4}$$

in which $\eta = \sqrt{\eta_1^2 + \eta_2^2} / e^2$, and here $\eta_1 = \eta_{11} + \eta_{22}$ and $\eta_2 = \sqrt{(\eta_{11} - \eta_{22})^2 + 4\eta_{12}^2}$; e is the eccentricity of the elliptical yield curve. Based on Eqs. (3) and (4), we have $\eta_{ij} = 0$ and $\eta_{ij} = \eta / e^2$ when the ice cover has a small shear rate ($P/2 > 0$). Under this condition, the ice cover exhibits linear viscous rheological characteristics. When the ice cover has a large shear rate ($P/2 < 0$), the ice principal stresses lie on the elliptical yield curve, and the ice cover displays plastic rheology.

The pressure term is calculated by (Shen et al., 1990)

$$P = \tan^2 \left(\frac{\alpha}{4} \pm \frac{\beta}{2} \right) \left(1 - \frac{c}{w} \right) \frac{g h_i}{2} \left(\frac{N}{N_{max}} \right)^j \tag{5}$$

where α is the internal friction angle of surface ice, N_{max} is the maximum possible ice concentration, and j is an empirical constant set to 15 normally. The "+" and "-" signs are for passive and active states of ice flow.

3. Modified PIC Method for Sea Ice Dynamics

In this modified PIC method, the ice cover is discretized into a series of ice particles, which have their own locations, velocities, thicknesses, concentrations and sizes. With the Gaussian kernel function, the ice information at a grid node can be interpolated from their surrounding ice particles. The ice velocity at a grid node is solved with FD method, and used to determine the ice particle velocity. With re-distribution of ice particles in the Lagrangian system, the mass density of ice particles will be adjusted to determine the particle thickness and the concentration of the ice particles.

3.1 Ice Thickness and Concentration at Eulerian Grid Node

The sea ice thickness and concentration at the Eulerian grid nodes can be interpolated with the Gaussian kernel function from their neighboring sea ice particles. Based on the SPH theory (Shen et al., 2000), a field variable f at position r can be expressed as:

$$\bar{f}(r) = \sum_{k=1}^N \frac{m_k}{M_k} f(r_k) W(r - r_k, h_0), \tag{6}$$

where r is the position vector for estimating variable f , r_k is the position vector of ice particle k , M_k and m_k are mass density and mass of particle k , and h_0 is the smooth length, which determines the range of influence of the interpolation kernel. In this study, the Gaussian kernel foundation is adopted, which has good continuity and precision as the interpolating function. The spatial distribution of the 2D Gaussian kernel function is plotted in Fig. 1, and can be written as:

$$W(r - r_k, h_0) = \frac{1}{h_0^2} \exp\left[-\frac{(r - r_k)^2}{h_0^2}\right]. \tag{7}$$

Based on Eq. (6), the ice thickness and concentration at grid node $X_{i,j}$ can be determined from its neighboring ice particles by

$$\tilde{h}_i(X_{i,j}) = \sum_{k=1}^N \left[\frac{m_k}{M_k} W(X_{i,j} - r_k, h_0) h_i(r_k) \right], \tag{8}$$

$$\tilde{N}_i(X_{i,j}) = \sum_{k=1}^N \left[\frac{m_k}{M_k} W(X_{i,j} - r_k, h_0) N(r_k) \right], \tag{9}$$

where $X_{i,j}$ is the position vector of the grid node; $h_i(r_k)$ and $N(r_k)$ are the thickness and concentration of ice particle k ; $\tilde{h}_i(X_{i,j})$ and $\tilde{N}_i(X_{i,j})$ are the estimated thickness and concentration at grid node $X_{i,j}$.

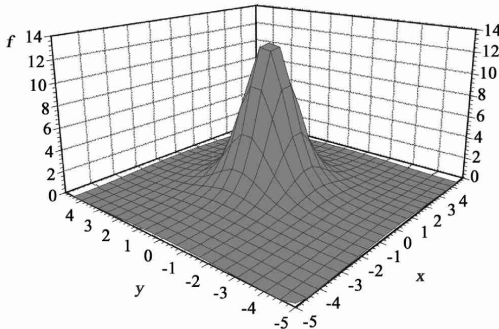


Fig. 1. Sketch of spatial distribution of 2D Gaussian function.

3.2 Sea Ice Velocity at Eulerian Grid Node

The ice velocity at a grid node can be calculated from the sea ice momentum equation with Eulerian FD method. The components in x and y directions of the sea ice momentum equation can be written as:

$$\begin{cases} \frac{\partial U}{\partial t} + U \frac{\partial U}{\partial x} + V \frac{\partial U}{\partial y} = fV - g \frac{\partial w}{\partial x} + (a_x + w_x + F_x) / M \\ \frac{\partial V}{\partial t} + U \frac{\partial V}{\partial x} + V \frac{\partial V}{\partial y} = -fU - g \frac{\partial w}{\partial y} + (a_y + w_y + F_y) / M \end{cases} \tag{10}$$

where, U and V are ice velocities in x and y directions; a_x and a_y , w_x and w_y are the components of air and water drag stress; F_x and F_y are internal ice force components, which can be determined by

$$F_x = \frac{\partial}{\partial x}(\tau_{xx}h) + \frac{\partial}{\partial y}(\tau_{xy}h), \quad F_y = \frac{\partial}{\partial y}(\tau_{yy}h) + \frac{\partial}{\partial x}(\tau_{yx}h), \tag{11}$$

in which, $\dot{\sigma}_{xx}$, $\dot{\sigma}_{yy}$, $\dot{\sigma}_{xy}$ and $\dot{\sigma}_{yx}$ are the ice stress components. Based on the viscous plastic constitutive model of Hibler (1979), the sea ice stresses can be written as:

$$\begin{cases} \dot{\sigma}_{xx} = \dot{\sigma}_{xx} + \dot{\sigma}_{xx} + \dot{\sigma}_{yy} - \dot{\sigma}_{yy} - \frac{P}{2} \\ \dot{\sigma}_{yy} = \dot{\sigma}_{yy} + \dot{\sigma}_{xx} + \dot{\sigma}_{yy} - \dot{\sigma}_{xx} - \frac{P}{2} \\ \dot{\sigma}_{xy} = \dot{\sigma}_{yx} = 2 \dot{\sigma}_{xy} \end{cases} \quad (12)$$

where, $\dot{\sigma}_{xx}$, $\dot{\sigma}_{xy}$ and $\dot{\sigma}_{yy}$ are strain rate components.

In the present study, the FD method has a spatial central difference scheme with a staggered grid and a three level time difference scheme (Fig. 2). In the first half time step from $n \ t \ (n + 1/2) \ t$, the velocity component in x direction, $U_{i+1/2,j}^{n+1/2}$, is solved with an implicit scheme, and the velocity component in y direction, $V_{i,j+1/2}^{n+1/2}$, is solved with an explicit scheme. In the second half time step from $(n + 1/2) \ t \ (n + 1) \ t$, the velocities, $V_{i,j+1/2}^{n+1}$ and $U_{i+1/2,j}^{n+1}$, are solved with implicit and explicit schemes in y and x directions, respectively.

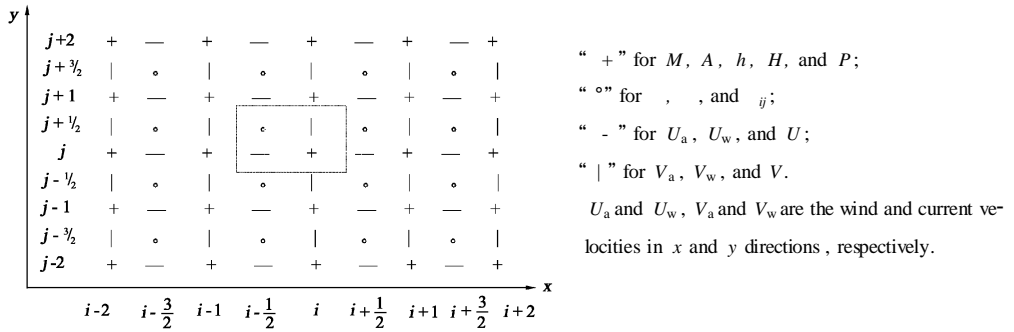


Fig. 2. Coordinate of difference cell for sea ice momentum equation.

3.3 Velocity and Position of Sea Ice Particle

With the ice velocity $(U_{i+1/2,j}, V_{i,j+1/2})$ at a grid node solved with FD method at time t^n or $t^{n+1/2}$, the velocity vector of ice particle k , $\tilde{V}(r_k(t^n))$ or $(U(r_k), V(r_k))$ can be estimated from the velocities at its neighboring grid nodes, and can be written as:

$$\tilde{U}(r_k) = \sum_{i,j} \left[\frac{m_{i,j}}{M_{i,j}} W(X_{i,j} - r_k, h_0) U_{i+1/2,j} \right] \quad (13)$$

$$\tilde{V}(r_k) = \sum_{i,j} \left[\frac{m_{i,j}}{M_{i,j}} W(X_{i,j} - r_k, h_0) V_{i,j+1/2} \right] \quad (14)$$

where, $\tilde{U}(r_k)$ and $\tilde{V}(r_k)$ are the velocity components in x and y directions of ice particle k , respectively; $U_{i+1/2,j}$ and $V_{i,j+1/2}$ are the sea ice velocity components at the grid node; $m_{i,j}$ and $M_{i,j}$ are the mass and mass density of grid; h_0 is the smooth length. Here we have $h_0 = \frac{1}{2}(\Delta x + \Delta y)$, Δx and Δy being the grid size in x and y directions, respectively.

The velocity vector of sea ice particle k at time $t^{n+1/2}$ or t^{n+1} can be determined with Eqs. (13) and (14). If its location vector at time t^n is $r_k(t^n)$, then its position vector $r_k(t^{n+1/2})$ at time $t^{n+1/2}$ can be calculated with

$$r_k(t^{n+1/2}) = r_k(t^n) + \frac{t}{2} \tilde{V}(r_k(t^n)), \tag{15}$$

where t is the time step.

3.4 Thickness and Concentration of Sea Ice Particles

In a previous PIC study for sea ice dynamics, Flato (1993) interpolated the ice thickness and concentration at grid nodes from the volume and area of ice particles. And the ice particle area was adjusted based on the feedback of the estimated concentration in cells with the critical condition $N_{\max} = 1.0$. Huang and Savage (1998) determined the physical ice thickness in cells with its continuity equation by FD method, then determined the mean ice thickness in cells with interpolation from ice particle thicknesses. The ice concentration at the cell centers was evaluated with $N = h/h_p$. In the present study, the mass density and smooth length of ice particles are introduced for the calculation of thickness and concentration of particles. Then, the thickness and concentration in cells can be interpolated from the thickness and concentration of particles.

If the ice particle k has position vector r_k , its mass density can be estimated from its neighboring particles,

$$\tilde{M}(r_k) = \sum_{j=1}^N m_j W(r_k - r_j, h_0). \tag{16}$$

The smooth length h_0 has a close relationship with mass density. If the initial smooth length is $h_0^{(0)}$, its smooth length at n -th time step can be determined with

$$h_0^{(n)} = h_0^{(0)} \left(\frac{M^{(0)}}{M^{(n)}} \right)^{\frac{1}{2}} \tag{17}$$

where $h_0^{(0)}$ and $h_0^{(n)}$ are the initial smooth length and the smooth length at time step n ; $M^{(0)}$ and $M^{(n)}$ are the initial mass density and the mass density at time step n .

The mass density of particle k can also be written as $\tilde{M}(r_k) = \sum_i N(r_k) h_i(r_k)$, and its concentration can be determined by

$$N(r_k) = \frac{\tilde{M}(r_k)}{\sum_i h_i(r_k)}. \tag{18}$$

If the simulated ice concentration $N(r_k) > 1.0$, ice ridging or rafting will occur. In this situation, we set $N(r_k) = N_{\max} = 1.0$, and have the ice thickness $h_i(r_k) = \tilde{M}(r_k) / (\sum_i N_{\max})$.

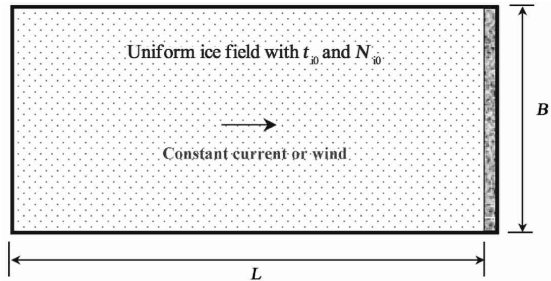
With the above modified PIC method, the sea ice dynamics can be simulated in the first half time step from t^n to $t^{n+1/2}$ or the second half time step from $t^{n+1/2}$ to t^{n+1} . In this method, a Gaussian kernel function is used to interpolate the ice variables between Lagrangian particles and Eulerian grids. The thickness and concentration of ice particles are determined with their smooth length and mass density. With the modified PIC method, the sea ice dynamics could be modeled without numerical diffu

sion. Its computational cost is lower than that of the SPH method for its does not have the complex interpolation in the calculation of ice particle interactions.

4. Numerical Simulation of Ice Ridging in A Regular Domain

Under constant wind and current drags, the ice ridging process in a rectangular domain is simulated for verification of the modified PIC method. The initial ice condition is that ice of thickness t_{i0} and concentration N_{i0} is distributed uniformly over a rectangular region of length L and width B , as shown in Fig. 3. Under constant wind and current drags, the ice cover will pile up at the downstream end. The internal ice resistance increases with the ice thickness to balance the wind and current drag forces. In the steady state, the ice strain rate $\dot{\epsilon}_{ij} = 0$, and the ice concentration approaches its maximum value, i.e. $N_{max} = 1.0$. In this simulation, the gravitational gradient and the Coriolis effect are both ignored.

Fig. 3. Sketch of the initial distribution of sea ice over the regular region.



With the smooth boundary, the analytical solution for the thickness profile of the static ice ridge can be obtained as (Shen et al., 2000):

$$t_i = \sqrt{t_{i0}^2 + \frac{2(C_a C_a V_a^2 + C_w C_w V_w^2)}{\tan^2\left(\frac{\pi}{4} + \frac{\phi}{2}\right) \left(1 - \frac{\rho_i}{\rho_w}\right) \rho_i g} x} \tag{19}$$

where t_{i0} is the single layer ice thickness at the ice edge, and x is the distance from the leading edge to the ice ridge, where $t_i = t_{i0}$.

In this numerical test of ice ridging, the initial ice region $L \times B = 20 \text{ km} \times 20 \text{ km}$, the initial thickness $t_{i0} = 0.2 \text{ m}$, and the initial concentration $N_0 = 100 \%$. The current velocity is set at zero, the wind velocity is 15 m/s , and the wind direction is 270° . In the simulation, the time step $\Delta t = 9.0 \text{ s}$, the grid size $\Delta x \times \Delta y = 400 \text{ m} \times 400 \text{ m}$, and there are 2×2 particles in a cell initially.

The wind and current drags are the main driving forces in the sea ice dynamics, and the drag coefficients are the most important in their calculation. The wind and current drag coefficients vary with different sea ice conditions. Based on the results for different regions and the sea ice characteristics in the Bohai Sea (Ji et al., 2003), we adopt the wind coefficient $C_a = 0.0015$ and the current coefficient $C_w = 0.0045$, respectively. The main parameters are listed in Table 1.

Table 1 Parameters used in the ice ridging simulation

| Parameter | Value | Parameter | Value |
|-----------------------|---|--------------------------|---|
| Ice frictional angle | $= 46^\circ$ | Bulk viscosity | $\mu_0 = 1.0 \times 10^6 \text{ N} \cdot \text{s} / \text{m}^2$ |
| Air density | $\rho_a = 1.29 \text{ kg} / \text{m}^3$ | Shear viscosity | $\mu_0 = 2.5 \times 10^5 \text{ N} \cdot \text{s} / \text{m}^2$ |
| Wind drag coefficient | $C_a = 0.0015$ | Current drag coefficient | $C_w = 0.0045$ |
| Water density | $\rho_w = 1010 \text{ kg} / \text{m}^3$ | Ice density | $\rho_i = 910 \text{ kg} / \text{m}^3$ |

With the modified PIC method, the simulated width-averaged thickness is plotted in Fig. 4. It can be seen that, under the given wind in the 270° direction, the ice ridging approaches the steady state in 14 hours, and the mean ice thickness is consistent with the analytical solution. The measured results for the Bohai Sea show that the level ice thickness is generally smaller than 0.2 m, and the rafted ice thickness can be over 0.4 m. In general, the thickness of the hummocked ice is 1 ~ 2 m, and its maximum value can be 3 ~ 5 m (Wu et al., 2001). The ridge height in this sample is 1.31 m, which is reasonable based on measured data for the Bohai Sea.

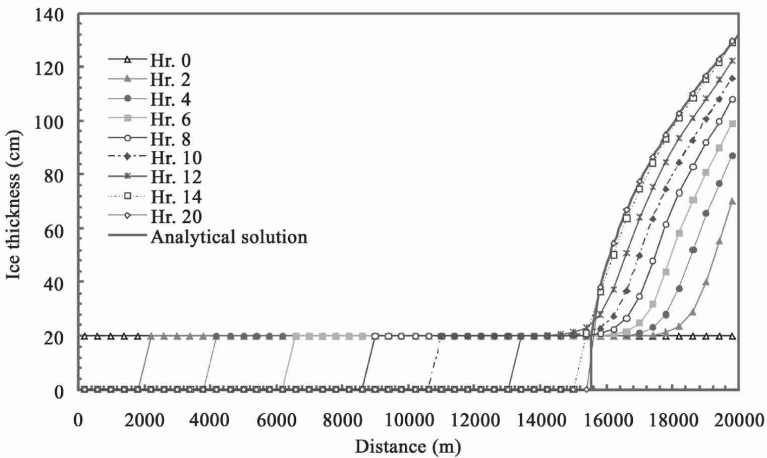


Fig. 4. Comparison of simulated result with analytical solution in static ice ridge thickness profile.

For the wind direction of 225° , the simulated ice thickness contour and the ice velocity vector are shown in Fig. 5. It can be found that, under the wind drag, the ice cover ridges at the downwind corner of the domain. In 20 hours, the ice ridge approaches a steady state.

5. Simulation of Sea Ice in the Bohai Sea

To examine the validity of the modified PIC method, we simulate the sea ice dynamics of the Liaodong Bay for 72 hours from 13:40, Jan. 22, 2004, and compare the results with the satellite remote sensing image and field data. The initial ice thickness and concentration are obtained from the digital NOAA remote sensing image, and displayed on the first picture in Figs. 6 and 7, respectively. The wind velocity measured at Jz20-2 platform ($121^\circ 21'$, $40^\circ 30'$) is used as the wind field in the

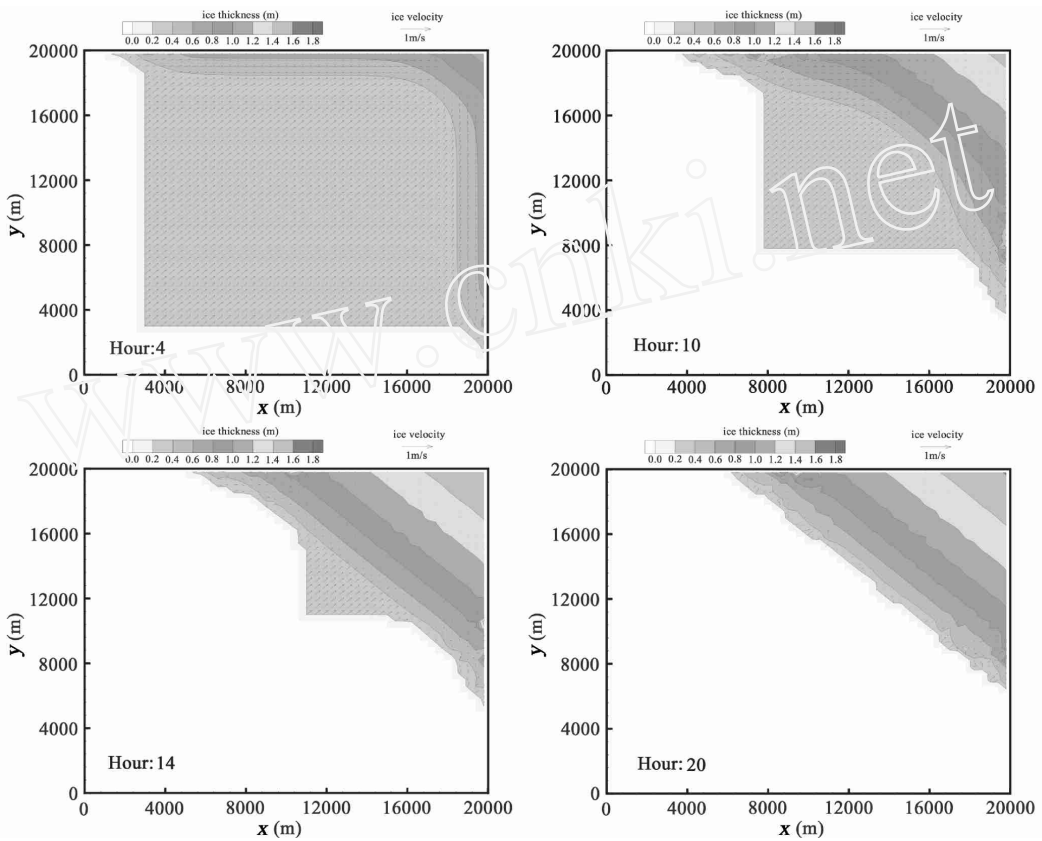


Fig. 5. Distributions of simulated ice velocity and ice thickness.

Liaodong Bay is assumed to be uniform. The tidal current is calculated with 2D shallow water equation by ADFFD algorithm. In the simulation, the time step is 600 s, the grid size is $0.1^\circ \times 0.1^\circ$, and there are 5×5 particles in one cell initially. The other computational parameters are listed in Table 1.

5.1 Simulated Ice Distribution in the Liaodong Bay

The ice thickness contours simulated with the modified PIC method for different times are plotted in Fig. 6. In this figure, the satellite remote sensing images are also given for comparison with the simulated results. It can be seen that the modified PIC can simulate the ice dynamics well. The simulated ice concentrations are mostly in the range from 80 % to 100 %, which can be found from Fig. 7. Within the 72 hours of numerical simulation, the simulated ice edge drifted to the south area under the north wind action, and the simulated ice concentration was decreased slightly. If the ice thermodynamics is considered in the model, the simulated results should be more reasonable.

5.2 Simulated Results for Jz20-2 Area of Liaodong Bay

The sea ice parameters for the Jz20-2 area of the Liaodong Bay are interpolated from its neighboring particles with the Gaussian function. The simulated ice thickness and velocity in the 72 hours are

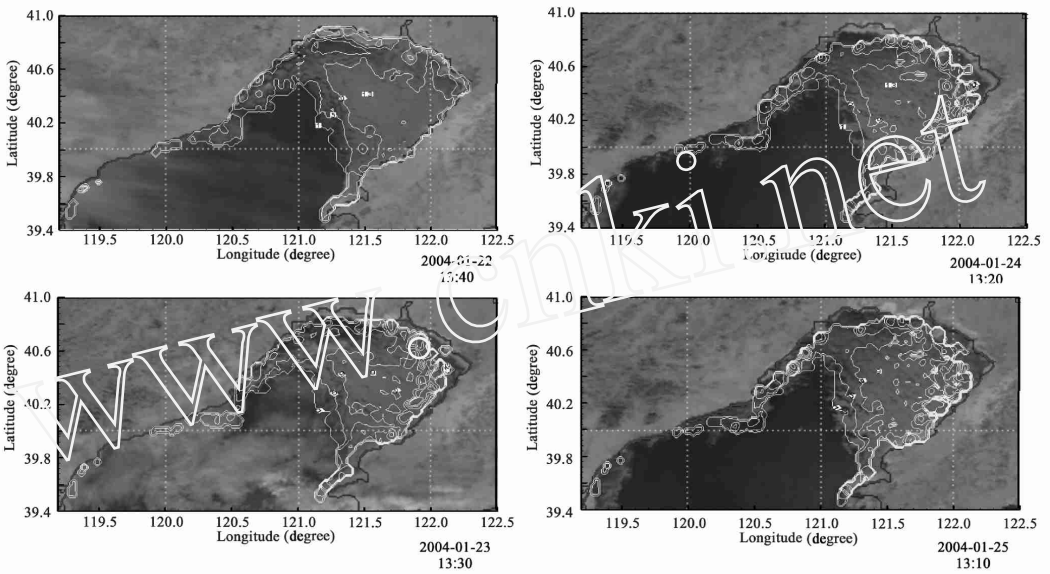


Fig. 6. Simulated ice thickness contour and satellite remote sensing image at different times.

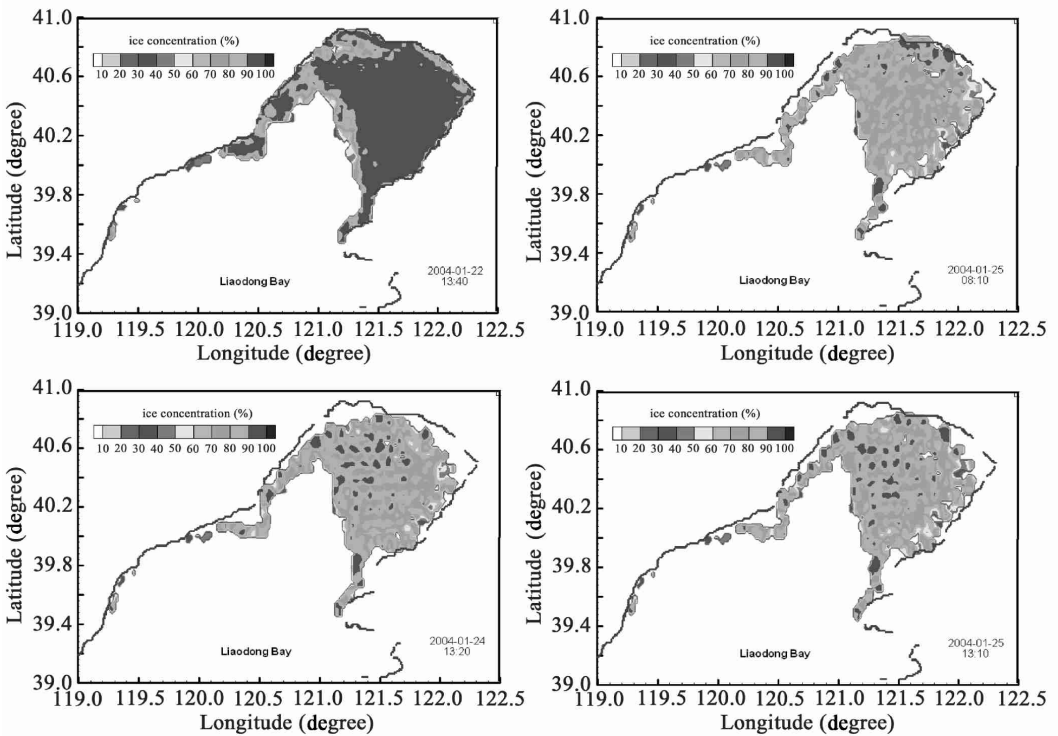


Fig. 7. Distributions of sea ice concentration simulated at different time steps.

plotted in Fig. 8. The ice information observed on the JZ20-2 oil/ gas platform is also plotted in this

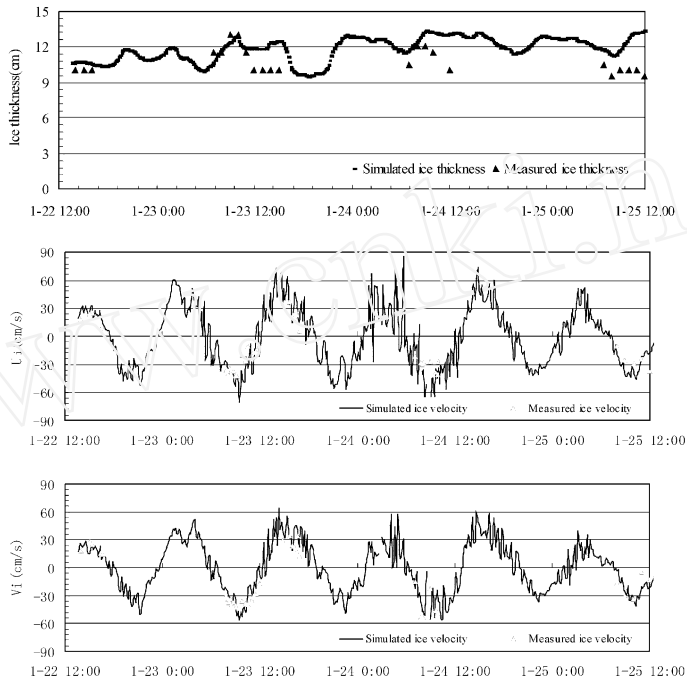


Fig. 8. Simulated and measured ice information for JZ20-2 area in 72 hours.

figure. It can be found that the observed ice thickness lies in the range from 9 cm to 13 cm, which is in agreement with the simulated data. Under the strong tidal current, the ice velocity displays a regular fluctuation, which can be observed from the simulated data. The simulated velocity is in good agreement with the field measured data.

6. Conclusion

In the numerical simulation of sea ice dynamics, it is very important to develop effective and accurate numerical methods. In this study, a modified particle-in-cell (PIC) method is developed coupling the Eulerian FD method and Lagrangian SPH model. In this modified PIC method, the Gaussian kernel function is adopted instead of the bi-linear function, and the mass density and the smooth length of ice particles are used to determine the particle thickness and concentration. In this way, the numerical diffusion of the Eulerian FD method can be avoided, and the Gaussian function with perfect continuity is more precise than the bi-linear function. The ice velocity at the Eulerian grid is simulated with finite difference method, and the movement of ice is determined under Lagrangian coordinate. The ice parameters are transferred between the Eulerian grid and Lagrangian ice floe by means of Gaussian interpolation. By use of the modified PIC method, the ice ridging process in a rectangular region and sea ice dynamics of the Bohai Sea are simulated, and the results are in good agreement with the analytical solution and observed data. The computation efficiency of the modified PIC is evidently higher than that of SPH. For instance, in the case of ice ridging, the computation time with the modified PIC is 15

minutes, while it is 50 minutes with SPH. The reason is that with the modified PIC, the sea ice stress and motion are calculated based on the Eulerian FD method, thus, the time step is much larger than that for the SPH calculation under Lagrangian coordinate. Therefore, both the computation efficiency and precision of the modified PIC method are high in the numerical simulation of sea ice dynamics.

Acknowledgements—The authors appreciate the study of REU student Katrina Ligett from Brown University, USA, and the helpful discussions with Prof. Hayley Shen and Dr. Lianwu Liu from Clarkson University, USA.

References

- Dai, M., Shen, H. H., Hopkins, M. A. and Ackley, S. F., 2004. Wave rafting and the equilibrium pancake ice cover thickness, *Journal of Geophysical Research*, **109**(C07023) : 1 ~ 9.
- Flato, G. M., 1993. A particle-in-cell sea-ice model, *Atmosphere Ocean*, **31**(3) : 339 ~ 358.
- Gutfrand, R. and Savage, S. B., 1997a. Marginal ice zone rheology: comparison of results from continuum plastic models and discrete-particle simulations, *J. Geophysical Research*, **102**(C6) : 12647 ~ 12661.
- Gutfrand, R. and Savage, S. B., 1997b. Smoothed Particle Hydrodynamics for the simulation of broken ice fields: Mohr-Coulomb Type rheology and frictional boundary conditions, *Journal of Computational Physics*, **134**, 203 ~ 215.
- Hibler, W. D., 1979. A dynamic and Thermodynamic sea ice model, *Journal Physical Oceanography*, **9**, 815 ~ 846.
- Hopkins, M. A., Frankenstein, S. and Thorndike, A. S., 2004. Formation of an aggregate scale in Arctic sea ice, *Journal of Geophysical Research*, **109**(C01032) : 1 ~ 10.
- Hopkins, M. A., 1998. Four stages of pressure ridging, *Journal of Geophysical Research*, **103**, 21883 ~ 21891.
- Hopkins, M. A., 1996. The effects of individual ridging events on the thickness distribution in the Arctic ice pack, *Cold Regions Science and Technology*, **24**, 75 ~ 82.
- Huang, Z. J. and Savage, S. B., 1998. Particle-in-cell and finite difference approaches for the study of marginal ice zone problems, *Cold Regions Science and Technology*, **28**, 1 ~ 28.
- JI Shunying, WANG Ruixue, BI Xiangjun and YUE Qianjin, 2003. Determining method of sea ice drag coefficient, *Journal of Glaciology and Geocryology*, **25**(S2) : 299 ~ 303. (in Chinese)
- Lepparanta, M. and Hibler, W. D., 1985. The role of plastic ice interaction in Marginal Ice Zone dynamics, *Journal of Geophysical Research*, **90**(C6) : 11899 ~ 11909.
- Lindsay, R. W. and Stern, H. L., 2004. A new Lagrangian model of Arctic sea ice, *Journal of Physical Oceanography*, **34**, 272 ~ 283.
- Lu, Q. M., Larsen, J. and Tryde, P., 1989. On the role of ice interaction due to floe collisions in marginal ice zone dynamics, *Journal of Geophysical Research*, **94**, 14525 ~ 14537.
- Overland, J. E., McNutt, S. L., Salo, S., Groves, J. and Li, S., 1998. Arctic sea ice as a granular plastic, *Journal of Geophysical Research*, **103**, 21845 ~ 21868.
- Shen, H. H., Hibler, W. D. and Lepparanta, M., 1987. The role of floe collisions in sea ice rheology, *Journal of Geophysical Research*, **92**(C10) : 7085 ~ 7096.
- Shen, H. T., Su, J. and Liu, L., 2000. SPH simulation of river ice dynamics, *Journal of Computational Physics*, **165**, 752 ~ 770.
- Tremblay, L. B. and Mysak, L. A., 1997. Modeling sea ice as a granular material, including the dilatancy effect, *Journal of Physical Oceanography*, **27**, 2342 ~ 2360.
- Wang, L. R. and Ikeda, M., 2004. A Lagrangian description of sea ice dynamics using the finite element method, *Ocean Modelling*, **7**, 21 ~ 38.
- WU Huiding, BAI Shan and ZHANG Zhanhai, 1998. Numerical simulation for dynamical processes of sea ice, *Acta Oceanologica Sinica*, **20**(2) : 1 ~ 13.
- WU Huiding, YANG Guojin et al., 2001. *Bohai sea ice design and operation conditions*, Beijing, China Ocean Press. (in Chinese)
- Zhang, J. and Hibler, W. D., 1997. On an efficient numerical method for modeling sea ice dynamics, *Journal of Geophysical Research*, **102**(C4) : 8691 ~ 8702.